

Baseline SUV_{max} is related to tumor cell proliferation and patient outcome in follicular lymphoma

Cédric Rossi,^{1,5} Marie Tosolini,^{1,3,6,7} Pauline Gravelle,^{1,4,6} Sarah Pericart,^{1,6} Salim Kanoun,⁸ Solene Evrard,⁶ Julia Gilhodes,⁹ Don-Marc Franchini,^{1,4} Nadia Amara,⁶ Charlotte Srykh,^{6, 10,11} Pierre Bories,^{10,11} Lucie Oberic,¹¹ Loïc Ysebaert,^{1,4,11} Laurent Martin,^{12,13} Selim Ramla,^{12,13} Philippine Robert,^{5,13} Claire Tabouret-Viaud,¹⁴ René-Olivier Casasnovas,^{5,13} Jean-Jacques Fournié,^{1,4} Christine Bezombes^{1,4*} and Camille Laurent^{1,4,6*}

¹Centre de Recherches en Cancérologie de Toulouse (CRCT), UMR1037 INSERM, Université Toulouse III Paul-Sabatier, ERL5294 CNRS, Toulouse; ²Laboratoire d'Excellence TOUCAN, Toulouse; ³Programme Hospitalo-Universitaire en Cancérologie CAPTOR, Université Toulouse, Toulouse; ⁴CALYM Carnot Institute, Pierre-Bénite; ⁵CHU Dijon, Hématologie Clinique, Hôpital François Mitterrand, Dijon; ⁶Département de Pathologie, Institut Universitaire du Cancer de Toulouse, Université Toulouse, Toulouse; ⁷Pôle Technologique du Centre de Recherches en Cancérologie de Toulouse, Toulouse; ⁸Médecine Nucléaire, Institut Universitaire du Cancer Toulouse-Oncopole, Université Toulouse, Toulouse; ⁹Bureau des Essais Cliniques, Institut Universitaire du Cancer Toulouse-Oncopole, Université Toulouse, Toulouse; ¹⁰Réseau Régional de Cancérologie, Onco-Occitanie, Institut Universitaire du Cancer, Université Toulouse, Toulouse-Oncopole; ¹¹Service d'Hématologie, Institut Universitaire du Cancer de Toulouse, Université Toulouse Toulouse; ¹²Département de Pathologie, CHU Hôpital François Mitterrand, Dijon; ¹³INSERM UMR 1231 UFR, Bourgogne and ¹⁴Département de Médecine Nucléaire, Centre Georges-François Leclerc, Dijon, France

*CB and CL contributed equally as co-senior authors.

ABSTRACT

Follicular lymphoma (FL) is the most common indolent lymphoma. Despite the clear benefit of CD20-based therapy, a subset of FL patients still progress to aggressive lymphoma. Thus, identifying early biomarkers that incorporate positron emission tomography metrics could be helpful to identify patients with a high risk of treatment failure with rituximab. We retrospectively included a total of 132 untreated FL patients separated into training and validation cohorts. Optimal threshold of baseline whole-body maximum standardized uptake (SUV_{max}) was first determined in the training cohort (n=48) to predict progression-free survival (PFS). The PET results were investigated along with the tumor and immune microenvironment, which were determined by immunochemistry and transcriptome studies involving gene set enrichment analyses and immune cell deconvolution, together with the tumor mutation profile. We report that baseline SUV_{max}>14.5 was associated with poorer PFS than baseline SUV_{max}≤14.5 (hazard ratio =0.28; P=0.00046). Neither immune T-cell infiltration nor immune checkpoint expression were associated with baseline PET metrics. By contrast, FL samples with Ki-67 staining ≥10% showed enrichment of cell cycle/DNA genes (P=0.013) and significantly higher SUV_{max} values (P=0.007). Despite similar oncogenic pathway alterations in both SUV_{max} groups of FL samples, four out of five cases harboring the infrequent *FOXO1* transcription factor mutation were seen in FL patients with SUV_{max}>14.5. Thus, high baseline SUV_{max} reflects FL tumor proliferation and, together with Ki-67 proliferative index, can be used to identify patients at risk of early relapse with rituximab chemotherapy.



Ferrata Storti Foundation

Haematologica 2022
Volume 107(1):221-230

Correspondence:

CHRISTINE BEZOMBES
christine.bezombes@inserm.fr

CAMILLE LAURENT
laurent.camille@iuct-oncopole.fr

CÉDRIC ROSSI
cedric.rossi@chu-dijon.fr

Received: June 24, 2020.

Accepted: December 11, 2020.

Pre-published: December 17, 2020.

<https://doi.org/10.3324/haematol.2020.263194>

©2022 Ferrata Storti Foundation

Material published in *Haematologica* is covered by copyright. All rights are reserved to the Ferrata Storti Foundation. Use of published material is allowed under the following terms and conditions:

<https://creativecommons.org/licenses/by-nc/4.0/legalcode>.

Copies of published material are allowed for personal or internal use. Sharing published material for non-commercial purposes is subject to the following conditions:

<https://creativecommons.org/licenses/by-nc/4.0/legalcode>, sect. 3. Reproducing and sharing published material for commercial purposes is not allowed without permission in writing from the publisher.



Introduction

Although some patients exhibit long-term remission after anti-CD20-based therapy, 20-30% patients with follicular lymphoma (FL) experience early progression,¹ and FL transforms into aggressive lymphoma in 2-3% patients per year.² Determining the prognostic factors that could be used in the early stages to identify patients with a high risk of treatment failure has become a central challenge in the management of FL.³ Follicular Lymphoma International Prognostic Index (FLIPI) and FLIPI2 scores, which include baseline clinical and standard biological parameters, are not able to accurately identify early relapse associated with an increased risk of death. Because FL is fluorodeoxyglucose (FDG) avid, FDG positron emission tomography (PET) is used in routine practice to stage pretreatment disease and to identify sites with high FDG uptake that are at risk of transformation.⁴ The predictive power of post-induction PET status on outcome appears to be much stronger than FLIPI or FLIPI2 scores and computed tomography (CT)-based response, and most patients who achieve PET negativity can expect their first remission to last several years.⁵ However, the critical challenge is to identify patients who have a high risk of standard treatment failure before initiating therapy.

Among baseline PET metrics, total metabolic tumor volume (TMTV) is a strong predictor of outcome in FL, independent from FLIPI2.⁶ Baseline whole-body maximum standardized uptake (SUV_{max}) has been used to predict outcomes in mantle cell lymphoma patients,⁷ but to our knowledge the value of pre-treatment SUV_{max} for prognosis in FL patients treated with rituximab (R)-chemotherapy followed by R maintenance (Rm) remains unclear. Very recently, a retrospective study⁸ reported that pre-treatment $SUV_{max} > 18$ was associated with lower overall survival (OS) in a cohort of 346 advanced stage FL patients, but only a few these patients received heterogeneous induction treatments with maintenance therapy.

The biological basis of high SUV_{max} at baseline remains unclear, and the cell populations, either in tumors or their microenvironment, that mediate a high uptake of FDG remain unknown. However, a pro-tumor microenvironment and its interactions with cancer cells could play a key role in promoting tumor cell growth and invasion.⁹ Recently, we developed a set of 33 genes involved in tumor immune escape (Immune Escape Gene Set [IEGS33]). IEGS33 includes the genes encoding for immune checkpoints (ICP) (e.g., *CTLA4*, *PDCD1*, *LAG3*, *HAVCR2*), for their ligands (e.g., *CD80*, *CD86*, *CD274*, *PDCD4LG2*, *LGALS9*), for enzymes producing immunosuppressive metabolites (e.g., *IDO1*, *ARG1*, *ENTPD1*), and for immunosuppressive cytokines and chemokines (e.g., *IL10*, *HGF*, *GDF15*). We discovered that the whole IEGS33 gene set is significantly up-regulated in all non-Hodgkin lymphoma (NHL) samples.¹⁰ Although immune escape strategies in lymphoma may vary between individuals, our former analysis of 1446 B-NHL transcriptomes evidenced the consistent up-regulation of IEGS33 in B-cell lymphomas.¹⁰ Furthermore, because the activation of immune effectors represents the 'substrate' of immune escape (IE), our meta-analysis of both 'T-cell activation' (44 T-cell genes such as *IL2*, *CD28*, *ZAP70*, *LCK*) and IEGS33 outlined four different stages of IE. These stages are seen in NHL patients in whom immune activation and escape are not observed, those in whom both are observed, those with mostly

immune activation, and those with mostly immune escape. Patients from these four classes displayed correspondingly different rates of overall survival (OS). Along the same lines, another study identified a signature of 23 genes involved in tumor cell cycle events (B-cell development, DNA damage response, cell migration and cell cycle) and immune regulation, which was predictive of progression-free survival (PFS) and progression of disease within 24 months (POD24) in FL patients with a high tumor burden treated with R-chemotherapy plus maintenance.¹¹ The tumor cell mutation profile may also influence patient outcomes. For instance, in combination with the FLIPI score, the mutation profile of seven genes (m7-FLIPI) involved in B-cell lymphomagenesis has been used to define a clinico-genetic risk index in FL patients receiving R-chemotherapy combined with cyclophosphamide, doxorubicin, vincristine and prednisone (R-CHOP).¹² So far, however, none of these expression and mutational signatures has been analyzed with regard to baseline PET metrics.

PET has become an important tool for staging and response assessment in FL patients. For this reason, the relationships between the molecular and functional imaging parameters need to be explored in order to ascertain whether they could improve FL patient risk stratification in the initial staging. The objective of our study was therefore to determine the prognostic value of PET metrics at baseline in FL patients, and to establish links to the molecular signatures of FL tumor cells and their immune cell infiltration.

Methods

Patients

The training cohort consisted of 48 FL patients (diagnosed by CL, CS or SP according to the World Health Organization classification¹³) treated in the Department of Hematology of the IUCT Oncopole (Toulouse, France) between 2011 and 2016. The validation cohort included 84 additional FL patients (diagnosed by LM or SR) treated in the Department of Hematology of the Dijon Bourgogne University Hospital (France) between 2012 and 2016. Patient characteristics are detailed in the *Online Supplementary Table S1*.

Tissue samples were collected and processed at the CRB Cancer des Hôpitaux de Toulouse and CRB Cancer du CHU de Dijon following ethics guidelines (Declaration of Helsinki), and written informed consent was obtained from all patients. CRB collections were declared to the Ministry of Research (DC-2009-989 for Toulouse, and DC-2008-508 for Dijon) and a transfer agreement (AC-2008-820) was obtained after approval from the appropriate ethics committees.

Positron emission tomography/computed tomography acquisition and analysis

Baseline PET acquisition was performed before any treatment and detailed in the *Online Supplementary Methods*.

PET images at baseline were centrally reviewed by one experienced reader (SK), who was blinded to any medical information, and analyzed using the free open-source software, Beth Israel Plugin for Fiji (<http://petctviewer.org>). PET and CT images (single modality and fused images) were displayed in three axes with multi-planar reconstruction along with maximum intensity projection.

Pathological uptake was defined as an increased uptake of ¹⁸F-FDG over the physiological background. For each PET, whole-

body SUV_{max} was recorded. The whole-body SUV_{max} corresponded to the single hottest tumor voxel in the whole-body acquisition. In order to determine TMTV, we performed the calculation based on relative threshold (>41% SUV_{max} threshold as recommended by the European Association of Nuclear Medicine) using Beth Israel Plugin.¹⁴

Data mining and transcriptome analyses

For gene expression analysis, RNA was extracted from the available frozen tumor samples (n=38 of 48). cDNA was prepared from minimum 500 pg RNA per sample and hybridized on GeneChip Human Gene HTA 2.0 Affymetrix microarrays (Affymetrix UK Ltd.), by the Lyon University genomic facility ProfileXpert-LCMT (Lyon, France), were done according to the manufacturer's protocol. Data are available on the NCBI Gene Expression Omnibus website (<http://www.ncbi.nlm.nih.gov/geo/>): GEO dataset GSE148070. Details of the methods used are presented in the *Online Supplementary Methods*.

Histopathology and immunohistochemistry studies

Samples fixed in 10% buffered formalin were processed for routine histopathological and immunohistochemical (IHC) examination. The IHC slides were digitalized using Panoramic 250 Flash II digital microscopes (3DHISTECH, Budapest, Hungary). IHC staining was evaluated both via manual scoring and with an automated method using image analysis software (see details in the *Online Supplementary Methods*).^{15,16}

Mutation profile analysis with next-generation sequencing

After DNA extraction of 51 available FL FFPE (n=33 from training cohort and n=18 from validation cohort), samples were sequenced on an Illumina MiSeqDx using our lymphopanel of 43 genes involved in B-cell lymphomagenesis.¹⁷ Sequencing and data analysis was performed as previously described^{17,18} (see details in the *Online Supplemental Methods*).

Statistics analysis

PFS was defined as the time from the first cycle of immunochemotherapy to progression or death (event) or last follow-up/change of treatment (censored data). POD24 was defined as primary-refractory disease (less than partial response), progression, transformation or relapse within 24 months after diagnosis. OS was defined as the time from the start of therapy to death or last follow-up. All survival rates were estimated using the Kaplan-Meier method, and log-rank test were assessed using R software. Median follow-up was calculated with the Kaplan-Meier reverse method.¹⁹ Optimal cutoff to predict PFS was determined using the R 'Survival' package^{20,21} and log-rank test-based *P*-values. Indeed, the multiple tests performed by this package were corrected using the Benjamini-Hochberg method²² to control the false discovery rate (FDR) and determine the optimal threshold. For comparisons between groups, a normality test followed by a Wilcoxon test or Student's *t*-test were performed using R software. The compound linear and nonlinear relationship between Ki-67 percentage and SUV_{max} level was automatically examined by computing the maximal information coefficient (MIC) with an algorithm running the MINE method.²³

Results

Study population

A total of 132 patients were included in the study, with

48 patients in the training cohort and 84 in the validation cohorts. The median age of the whole population was 61.8 years old (range, 28-87 years) (*Online Supplementary Table S1*). Most patients had advanced clinical stages (84%); 54% had high risk and 34% had intermediate risk FLIPI. FL histological grade was grade 1-2 in 91% of cases. The treatments were comparable between groups, with mostly rituximab plus CHOP or CHOP-like and rituximab maintenance (89%). With a median of follow-up of 43.4 months (interquartile range [IQR] 25.4-65.3 month), ten patients died from progressive disease and three from a second malignancy.

SUV_{max} at baseline correlates with the risk of progression in follicular lymphoma patients

The median baseline SUV_{max} was 9.15 (range, 2.5-34.6; IQR 8.3-13.8) in our series of 132 patients (*Online Supplementary Table S2*). Baseline SUV_{max} was related neither to baseline TMTV (Pearson index=0.35) nor to the largest lymph node size (Pearson index=0.06). Baseline TMTV was related to the size of the largest mass assessed in 119 patients (Pearson index=0.76). It is worth noting that the SUV_{max} median of 12 FL grade 3A was not significantly different from that of FL grade 1-2. We determined that a SUV_{max} 14.5 was an accurate threshold (sensitivity of 0.95, specificity of 0.16, false positive rate of 0.59, and precision of 0.85) that was able to distinguish patients with different outcomes. Only 14% of patients (n=19) had SUV_{max}>14.5. Overall PFS was significantly lower in patients with SUV_{max}>14.5 than in those with SUV_{max}≤14.5 (HR= 0.28; *P*=0.00046), and 2-year PFS was 54% versus 86% (*P*=0.006). (Figure 1A, left and 1B). On univariate analysis, factors associated with PFS were SUV_{max} (*P*=0.0016), FLIPI (*P*=0.048), elevated lactate dehydrogenase (LDH) (*P*=0.022), and elevated B2 microglobulin (*P*=0.038). The type of treatment regimen (R-chemotherapy vs. anti-CD20-lenalidomide) and baseline TMTV had no effect on PFS (Figure 1A, right). In a multivariate Cox model (SUV_{max}, FLIPI, LDH, B2 microglobulin), SUV_{max} was the only factor retaining an independent prognostic value for PFS (HR=0.25; *P*=0.0066).

Twelve patients (25%) experienced disease progression within 24 months after the start of therapy. POD24 events were more common in the subset of patients with SUV_{max}>14.5 (55% of patients with SUV_{max}>14.5) than in those with SUV_{max}≤14.5 (15% of patients with SUV_{max}≤14.5). Median OS was 23.9 months for patients with SUV_{max}>14.5 and not reached for patients with low SUV_{max} (HR 0.37; *P*=0.06).

Baseline SUV_{max} does not correlate with immune infiltration

In order to investigate whether the immune infiltration signature in baseline biopsies was associated with an increased ¹⁸F-FDG uptake, we compared patients with SUV_{max}>14.5 and SUV_{max}≤14.5, and the immune profile determined by immunochemistry (IHC) and transcriptome approaches.

We first measured the sample enrichment score (SES) of both 'T-cell activation' and 'IEG533' gene sets in each transcriptome from our FL training cohort and from 1,446 NHL and normal lymphoid tissue downloaded from public cohorts available in GEO data set.^{8,19}

The 38 available frozen FL samples from our training cohort and 148 of the 1,446 NHL samples had a high score

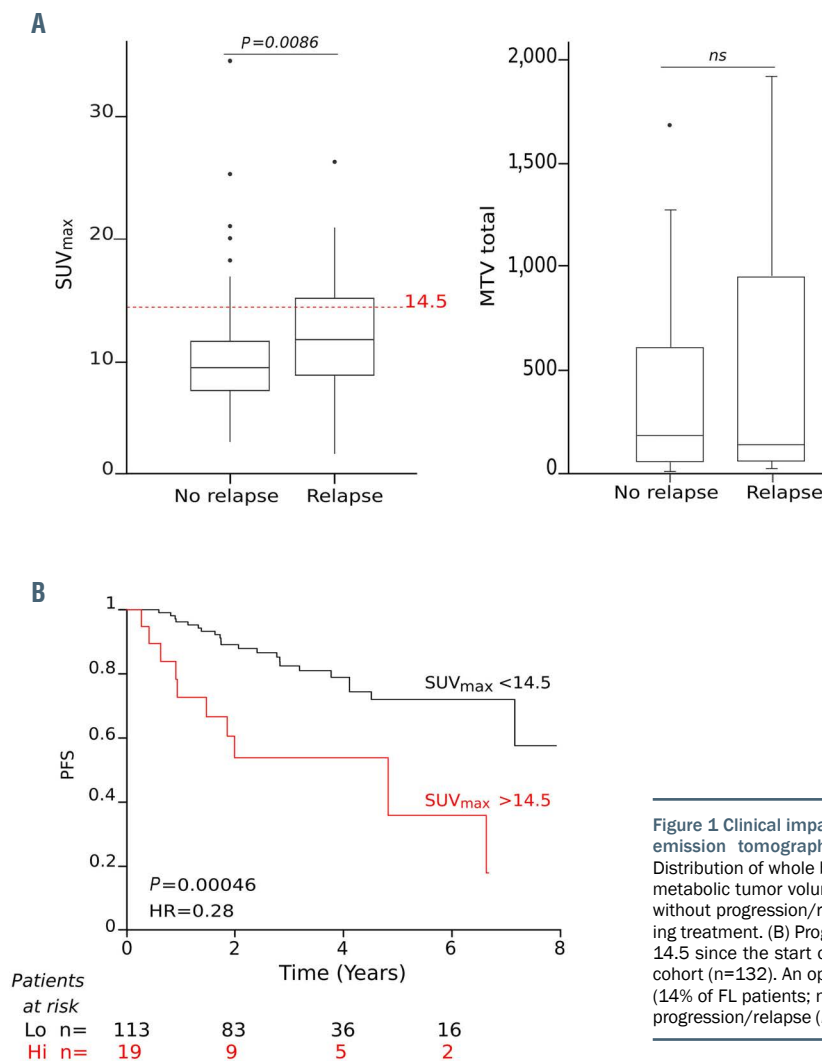


Figure 1 Clinical impact of SUV_{max} and total metabolic tumor volume at positron emission tomography baseline in the follicular lymphoma patients. (A) Distribution of whole body maximum standardized uptake (SUV_{max}) (left) and total metabolic tumor volume (TMTV) (right) in 132 follicular lymphoma (FL) patients without progression/relapse or with progression/relapse 24 months after starting treatment. (B) Progression-free survival (PFS) according to SUV_{max} threshold of 14.5 since the start of treatment. Kaplan-Meier estimates of PFS in the whole cohort (n=132). An optimal threshold was set to separate patients into high-risk (14% of FL patients; n=19 of 132) and low-risk (86%, n=113 of 132) groups for progression/relapse (P=0.00046). Hi: high SUV_{max}; HR: hazard ratio, Lo: low SUV_{max}.

for IEGS33, indicating up-regulation of immune escape genes. The score for T-cell activation signature in these FL samples was also among the highest. Finally, scatterplots of all samples for ‘IEGS33’ versus ‘T-cell activation’ showed that the FL samples clustered together, in contrast with most other NHL (Figure 2). These findings were confirmed upon datamining of another 160 FL samples from the PRIMA study²¹(*Online Supplementary Figure S1*).

In order to further characterize the IE status of FL samples at the protein level, FFPE samples were stained for ICP markers and were then scored. PD-1 expression in tumor-infiltrating lymphocytes (TIL) showed perifollicular, intrafollicular and diffuse patterns in 46%, 20% and 34% of cases, respectively. PD-1⁺ cells and PD-L1⁺ cells represented, respectively, 16% (range, 2-30%) and 5% (range, 2-10%) of CD3⁺ immune cells (Figure 3A). LAG3 staining was seen in less than 5% and TIM3 staining was seen in 15% of total CD3⁺ immune cells (ranging from 2% to 5% and from 5% to 15%, respectively). These results were consistent with those from transcriptomic analyses. All ICP protein expressions scored by IHC in each sample were strongly correlated with their respective IEGS33 scores (Figure 3B).

We then analyzed the correlation between baseline PET and molecular scores for IEGS and T-cell activation signa-

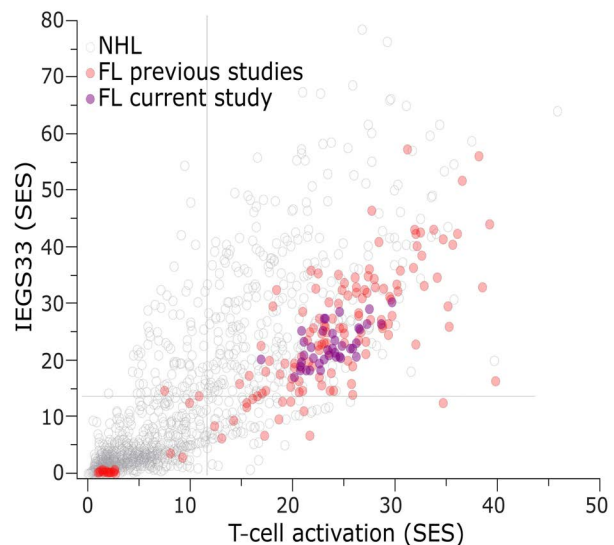


Figure 2. Functional immune status of follicular lymphoma samples from the training cohort and previously published lymphoma cohorts. Dot plot of sample enrichment scores (SES) for the immune escape gene set (IEGS33) versus T-cell activation gene set (defined in²⁰) in 38 frozen follicular lymphoma (FL) samples from our training cohort (purple dots) and 148 FL (red dots) among 1,446 non Hodgkin lymphoma (NHL) (grey dots) public microarrays datamining analysis.

tures in biopsies. However, no significant correlation emerged between immune escape/T-cell activation scores and baseline SUV_{max} or PFS (*Online Supplementary Figure S2*). In order to further assess the patterns of leukocyte infiltrates in the tumor samples, we performed algorithmic deconvolution by CIBERSORT to infer the proportion of 14 leukocyte and other non-hematopoietic cell types from each sample. At the same time, we assessed the immune cell composition of FL samples by IHC. Deconvolution of

bulk tumor transcriptomes unveiled a composition containing more CD8⁺ T lymphocytes and macrophages and fewer NK cells and $\gamma\delta$ T-cell cytolytic lymphocytes (*Online Supplementary Figure S3A*). Accordingly, the IHC analyses evidenced median percentages of CD3⁺T cells, CD8⁺ T cells and CD163⁺ monocytes of 35% (range, 5-60%), 14% (range, 1-40%), and 11% (range, 1-30%), respectively, of the total immune cell infiltrate (Figure 4A). The abundance of CD8⁺ T cells scored by IHC was high (>30% of immune

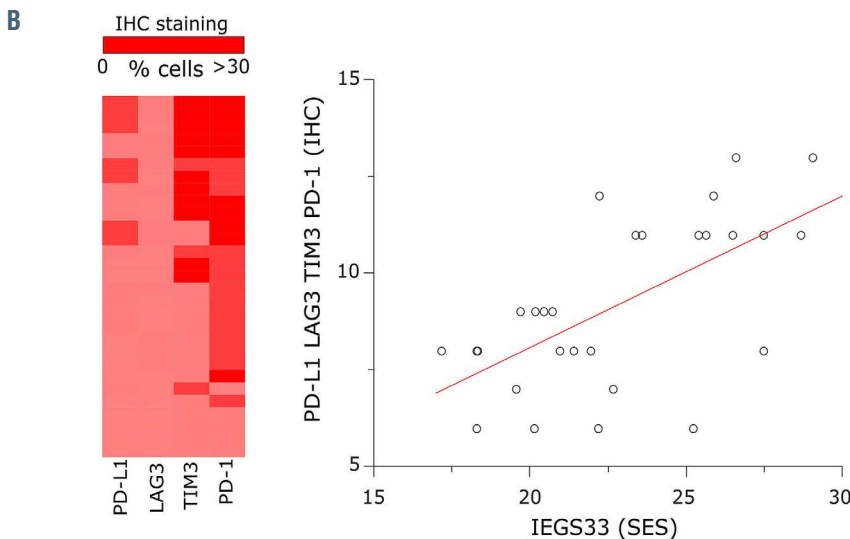
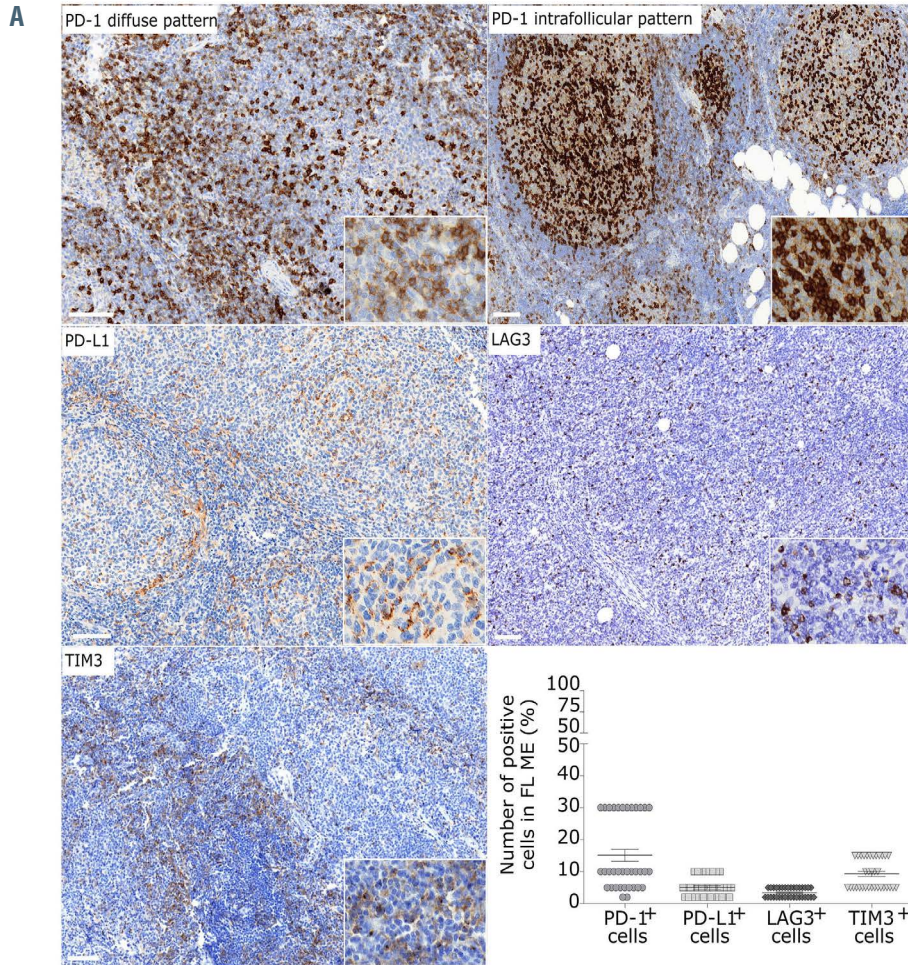


Figure 3. Immunohistochemical validation of immune escape gene set (IEGS33) overexpression in follicular lymphoma samples. (A) Upper panel shows a representative case of PD-1 staining with diffuse (left) intrafollicular (right) patterns (magnification: 100x and 50x, respectively and inserts: 200x). Medium panel shows representative cases of PD-L1 (left) and LAG3 (right) staining (magnification: 100x and inserts: 200x). Lower panel shows a representative case of TIM3 staining (left) (magnification: 100x and inserts: 200x) and immunohistochemical (IHC) quantification of immune checkpoint (ICP): PD-1, PD-L1, LAG3 and TIM3 staining (right). (B) The heat map (left) represents IHC scoring of the four ICP markers and the graph (right) shows the correlation between the percentage of ICP-positive immune cells scored by IHC and the sample enrichment scores (SES) for immune escape gene sets (IEGS) in each FL sample. Each sample is shown by a dot. FL: follicular lymphoma.

cells) in 20% of cases, low (<10%) in 40% cases, and intermediate (10-30%) in 40% of cases as illustrated in Figure 4B. The abundance of CD8⁺ T cells in FL correlated in the deconvolution and IHC results (Figure 4C). They also matched with T-cell activation scores, suggesting that transcriptomic evidence of T-cell activation in FL samples was consistent with and related to the cytotoxic CD8⁺ T cells observed by IHC (Figure 4C). By contrast however, the deconvoluted immune cell composition did not differ significantly according to SUV_{max} (Online Supplementary Figure S3B).

DNA repair/tumor proliferation signatures and SUV_{max}

We compared the tumor cell DNA repair/proliferation by transcriptomic and IHC approaches to ¹⁸F-FDG uptake signatures obtained. In the 38 available frozen FL samples, using the Gene Ontology (GO)²² and Reactome,²⁷ we scored the SES for gene signatures of tumor proliferation, such as GO cell cycle DNA, G2M DNA replication and base excision repair (BER), a pathway that increases with proliferative activity.²⁴ We observed a relationship between

the level of SUV_{max} and DNA repair/proliferation signature scores (Figure 5A; Online Supplementary Figure S4).

We then validated these findings at the protein level by scoring Ki-67 staining in FFPE samples. The Ki-67 staining was scored according to the percentage of Ki-67⁺ tumor cells determined by optical evaluation and quantified by automated image analysis solutions (Figure 5B). Using a cutoff value of 10%, Ki-67 immunostaining was found to be significantly associated with GO cell cycle DNA replication SES ($P=0.013$), BER SES ($P=0.0086$) and G2M checkpoint SES ($P=0.0059$) (Figure 5C). We then analyzed the correlation of PET-CT baseline and Ki-67 scoring. Using the MINE method²³ we found a non-correlated association between the quantitative variable of the SUV_{max} value and Ki-67 percentage estimated by automated quantification for the training cohort (MIC=0.59) and for the validation cohort (MIC=0.35). In addition, using the optimal Ki-67 cut-off of 10%, we found that the SUV_{max} level was significantly increased in FL grade 1-2 and 3A samples with Ki-67 staining $\geq 10\%$ (Wilcoxon $P=0.007$ in the training cohort and $P=0.006$ in the validation cohort) (Figure 5D). Finally,

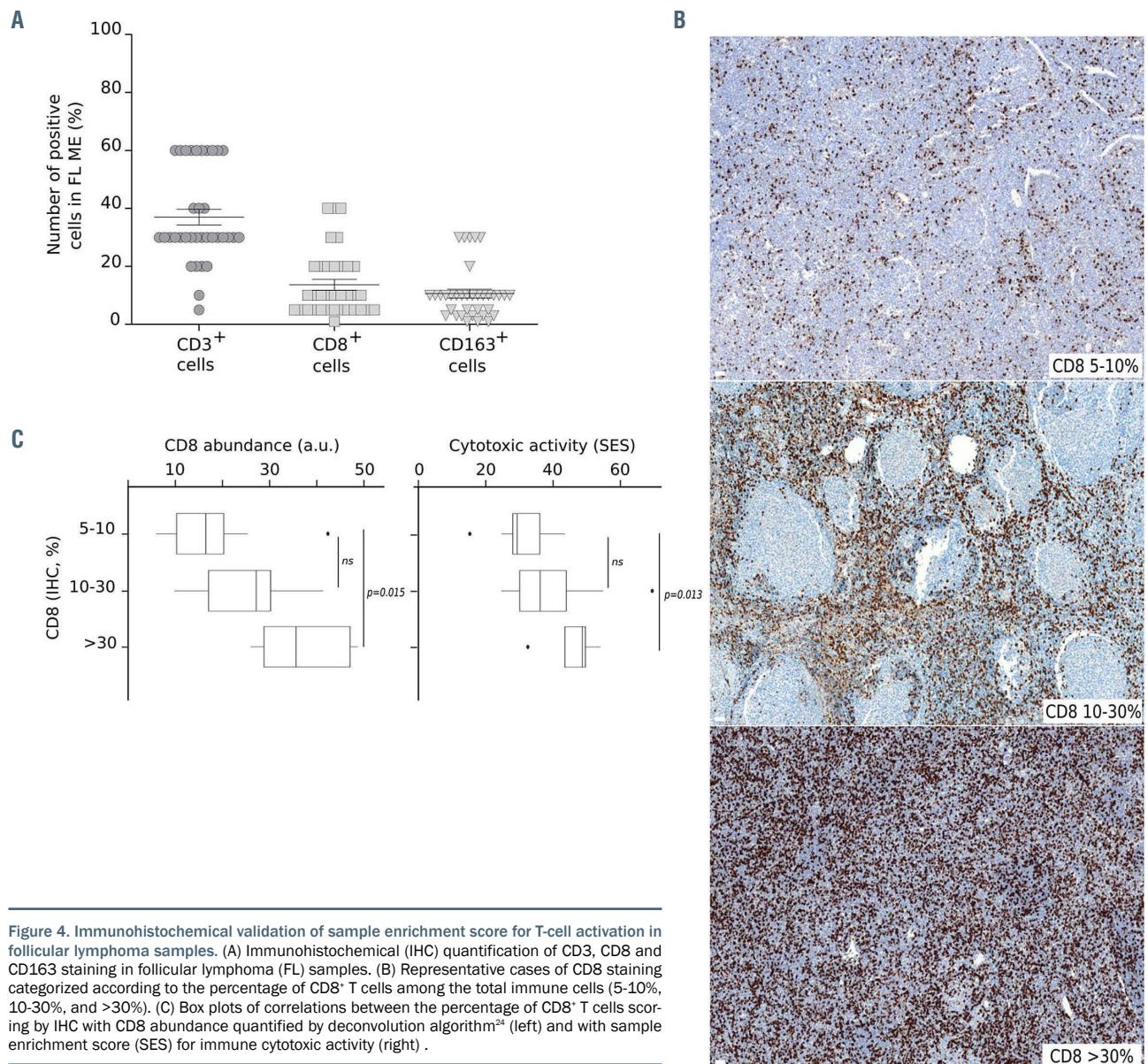


Figure 4. Immunohistochemical validation of sample enrichment score for T-cell activation in follicular lymphoma samples. (A) Immunohistochemical (IHC) quantification of CD3, CD8 and CD163 staining in follicular lymphoma (FL) samples. (B) Representative cases of CD8 staining categorized according to the percentage of CD8⁺ T cells among the total immune cells (5-10%, 10-30%, and >30%). (C) Box plots of correlations between the percentage of CD8⁺ T cells scoring by IHC with CD8 abundance quantified by deconvolution algorithm²⁴ (left) and with sample enrichment score (SES) for immune cytotoxic activity (right).

this SUV_{max}-to-Ki-67 index association suggests that ¹⁸F-DG uptake in FL patients at baseline reflects tumor cell proliferation.

Baseline SUV_{max} could be influenced by tumor cell mutation profiles

In the 33 available FL samples from the training cohort, targeted next-generation sequencing (NGS) identified 243 non-synonymous alterations in 32 genes (Figure 6A; *Online Supplementary Table S3*). The most frequently mutated genes were *KMT2D*, *CREBBP* and *BCL2* (22%, 14%, and 15% of total variants, respectively), which were detected in 82%, 73% and 58% of cases, respectively. A recurrent missense mutation in *EZH2* tyrosine 646 (Y646) was also found in 21% of cases. Altogether, 94% of patients harbored mutations involved in genes from epigenetic regula-

tion pathways (48.5% of total variants), whereas mutations in apoptotic pathways (16% of total variants) or in genes involved in immune response (21% of total variants) were less frequent (64% and 70% of patients) (Figure 6B). The mutational frequency in these altered pathways did not vary with the level of SUV_{max} (Figure 6C). However, *FOXO1* mutations (n=2 of 33) were exclusively detected in patients with high SUV_{max} (SUV_{max}>14.5), while *MFHAS1* (n=2), *MYC* (n=1), and *TP53* (n=6) mutations were only observed in patients with low SUV_{max} (SUV_{max}<6.5) (*Online Supplementary Figure S5*).

The same analyses in the validation cohort (n=18 available FL samples) unveiled 132 non-synonymous alterations in 32 genes. The most frequently mutated genes were *CREBBP*, *KMT2D* and *MEF2B* (18%, 13%, and 6% of total variants, respectively, occurring in 78%, 66%, and 44% of

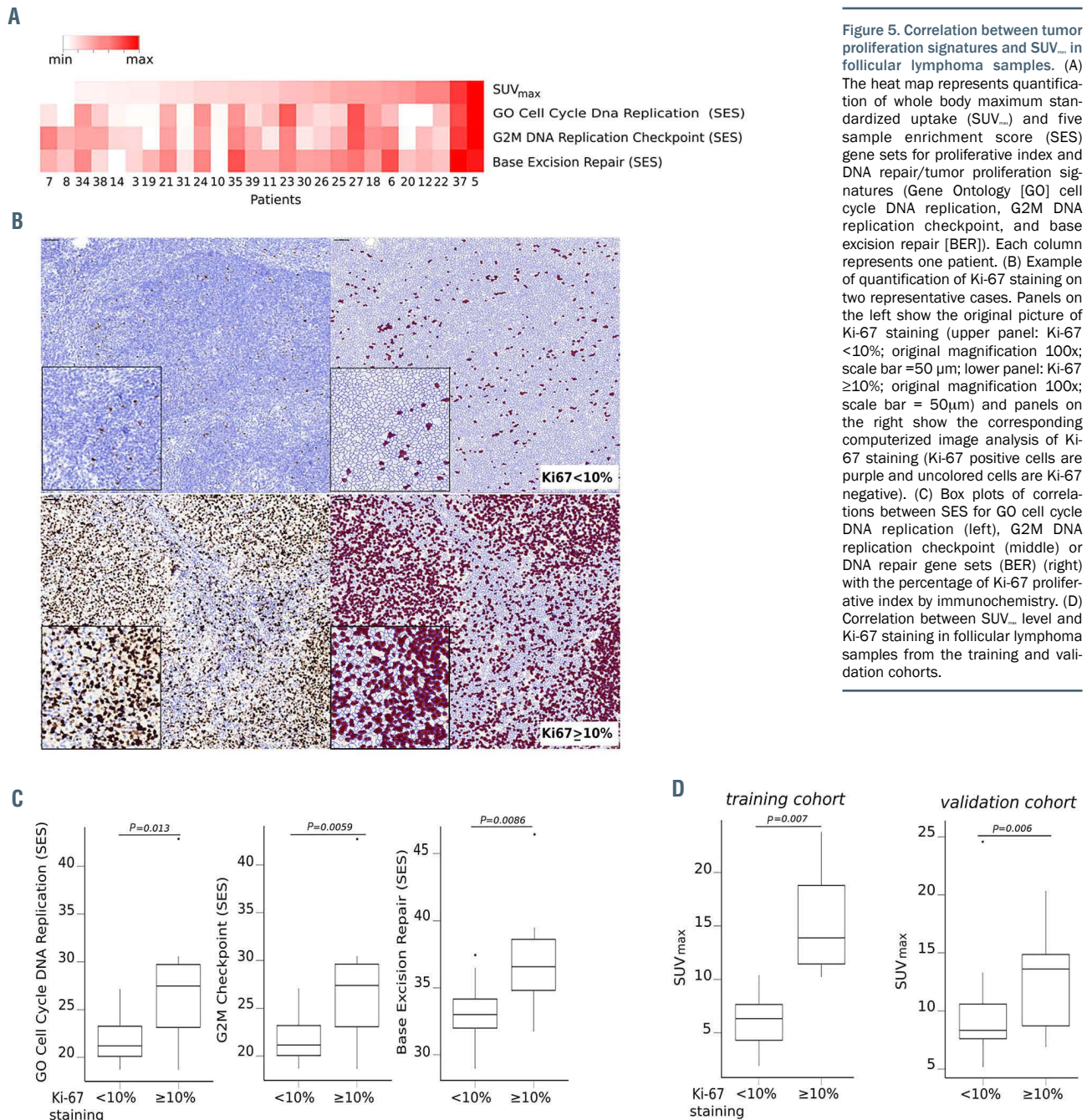


Figure 5. Correlation between tumor proliferation signatures and SUV_{max} in follicular lymphoma samples. (A) The heat map represents quantification of whole body maximum standardized uptake (SUV_{max}) and five sample enrichment score (SES) gene sets for proliferative index and DNA repair/tumor proliferation signatures (Gene Ontology [GO] cell cycle DNA replication, G2M DNA replication checkpoint, and base excision repair [BER]). Each column represents one patient. (B) Example of quantification of Ki-67 staining on two representative cases. Panels on the left show the original picture of Ki-67 staining (upper panel: Ki-67 <10%; original magnification 100x; scale bar =50 μm; lower panel: Ki-67 ≥10%; original magnification 100x; scale bar = 50μm) and panels on the right show the corresponding computerized image analysis of Ki-67 staining (Ki-67 positive cells are purple and uncolored cells are Ki-67 negative). (C) Box plots of correlations between SES for GO cell cycle DNA replication (left), G2M DNA replication checkpoint (middle) or DNA repair gene sets (BER) (right) with the percentage of Ki-67 proliferative index by immunochemistry. (D) Correlation between SUV_{max} level and Ki-67 staining in follicular lymphoma samples from the training and validation cohorts.

patients). Here again, alterations of epigenetic modifiers were the most frequent (41.7% of total variants occurred in 89% of patients) (Figure 6; *Online Supplementary Table S3*). Altogether, *FOXO1* mutations occurred in five FL patients (two from the training cohort and three from the validation cohort), four of which had $SUV_{max} > 14.5$.

Discussion

Our multi-parametric analysis of two independent cohorts of FL patients shows that baseline SUV_{max} values above 14.5 identified those with early unfavorable outcomes, defined here as poorer PFS and higher rate of POD24 events. Although this threshold is an absolute value which needs to be confirmed in larger cohorts, our study suggests that the overall high level of SUV_{max} at diagnosis could potentially reflect specific biological behaviors in FL tumors. Our results build on those recently obtained by Strati *et al.*⁸, who demonstrated the prognostic impact of baseline $SUV_{max} > 18$ in FL patients. Their use of a higher threshold could be explained by i) the more favorable dissemination of disease in the FL patients from our study (17% vs. 0% of Ann Arbor stage I-II)⁸, ii) the use of R-CHOP or other R-chemotherapy as induction treatment in our cohorts, while 15% of patients in Strati *et al.*⁸ received rituximab alone; iii) the fact that all of our patients received maintenance therapy while only few patients received Rm in Strati *et al.*⁸ and iv) PET acquisition and measures were performed on different PET/CT devices. These discrepancies suggest a better chance of disease control in our series, with a lower risk of relapse and fewer PFS events.^{25,28} Moreover, Strati *et al.*⁸ demonstrated a significant association between the largest lymph node ≥ 6 cm and $SUV_{max} > 18$. In our study, we focused on TMTV to assess the tumor burden seeing as available computed tomography was not mandatory for patient enrollment in the study. Nevertheless, for 119 (91%) patients with available computed tomography, the size of the largest lymph node was strongly related to TMTV but not to SUV_{max} . We found no correlation between the tumor burden and SUV_{max} in our series.

Pre-treatment PET staging is more sensitive than CT for identifying FL patients who have a high risk of transformation to aggressive lymphoma.²⁹ In line with our results, several other studies have suggested that SUV_{max} threshold values ranging from 10 to 13 could be used to identify FL with a higher risk of transformation.^{4,30,31} However, only tumor biopsy possibly guided by PET can rule out FL transformation into high grade lymphoma, which is *de facto* associated with reduced PFS and OS. Here, $SUV_{max} > 14.5$ did not necessarily indicate that FL would develop or transform into aggressive lymphoma. The biopsy sites used for FL diagnosis exhibited the higher SUV_{max} at PET baseline, while their histological analyses did not unveil any transformation. In our series, high avidity of FDG in FL samples was not associated with a specific infiltration pattern of major immune cell populations and was not correlated with increased of SES for IEGS33 and for T-cell activation gene set. Nevertheless, some FL samples lacked available frozen tissue for RNA sequencing and were unsuitable for further analyses. Our findings should thus be confirmed in a larger prospective cohort with sufficient biopsied material from the most FDG-avid FL tumor.

Moreover, the lack of association between tumor immunological contexture and prognosis could be related to anti-CD20 maintenance therapy, as already suggested.³² While baseline SUV_{max} appears unrelated to immune T-cell infiltration, it remains related to tumor cell proliferation, as shown by high DNA repair and Ki-67 proliferative indexes. Thus, these results suggest that $SUV_{max} > 14.5$ at baseline in FL patients with Ki-67 staining $\geq 10\%$ could define patients with high risk of relapse or progression. While TMTV, a surrogate marker of tumor cell burden, was unrelated to baseline SUV_{max} or patient outcomes in our series, TMTV > 510 cm³ has been associated with a higher risk of treatment failure in FL patients.⁶ However, this discrepancy could be related to the absence of maintenance treatment in the study by Meignan *et al.*⁶ Considering that the long-term results of the PRIMA study showed improved PFS in FL patients receiving rituximab maintenance (10.5 years compared to 4.1 years without maintenance treatment),³³ and the GALLIUM study³⁴ showed an additional benefit of obinutuzumab over rituximab for PFS, anti-CD20 maintenance could mitigate the prognostic value of TMTV at baseline. Accordingly, TMTV had no prognostic value in either arm (rituximab or obinutuzumab) of the GALLIUM study. This suggests that FL prognosis could be more related to the proportion of proliferating tumor cells than to the cell burden of the tumor. Ultimately, without evidence of transformation, high SUV_{max} in FL samples may be associated with more aggressive tumor cells. This has been observed in other low-grade lymphomas,³⁵ suggesting that the ability of FL tumors to proliferate may affect their avidity to FDG and thus the PET signals observed in FL patients.

The frequency of alterations in the oncogenic pathway did not vary with the SUV_{max} level, but we identified a *FOXO1* mutation in a subset of patients with $SUV_{max} > 14.5$. The prognostic value of *FOXO1* mutations has already been shown in DLBCL³⁶ and FL.^{12,37} For instance, *FOXO1* mutations were more frequently observed in high-risk FL patients with POD24 when compared with the non-POD24 subgroup (25% vs. 10%, $P=0.04$)^{12,37} and were associated with shorter failure-free survival (HR 2.74, range, 1.23-6.09; $P=0.013$) in the m7-FLIPI cohort.¹² Moreover, the *FOXO1* transcription factor appears to be implicated in the regulation of the abundance of CD20 on the surface of tumor cells, so alterations could influence the response to rituximab-based therapies as previously reported in an *in vitro* study of cell line assays.³⁸ On the contrary, we found certain mutations such as *TP53* and *MYC* more often in patients with $SUV_{max} < 14.5$. However, these observations could be related either to the spatial genetic heterogeneity of FL³⁹ or to possible areas of FL transformation.³⁹ In this context, high SUV_{max} levels could be very helpful to identify those FL sites with suspected transformation. That is why we selected lymph node biopsies with the most FDG-avid sites to ensure lack of transformation. However, single biopsy specimens cannot rule out transformation/genomic alteration or variation in other sites. Finally, baseline SUV_{max} outperformed FLIPI to predict patient outcomes, in addition to multi-biopsy site assessment of gene mutation profile; it could therefore possibly be used to identify patients who are at risk of poor outcomes.

In conclusion, $SUV_{max} > 14.5$ at baseline FDG-PET is associated with poor PFS and high risk of POD24 events in FL

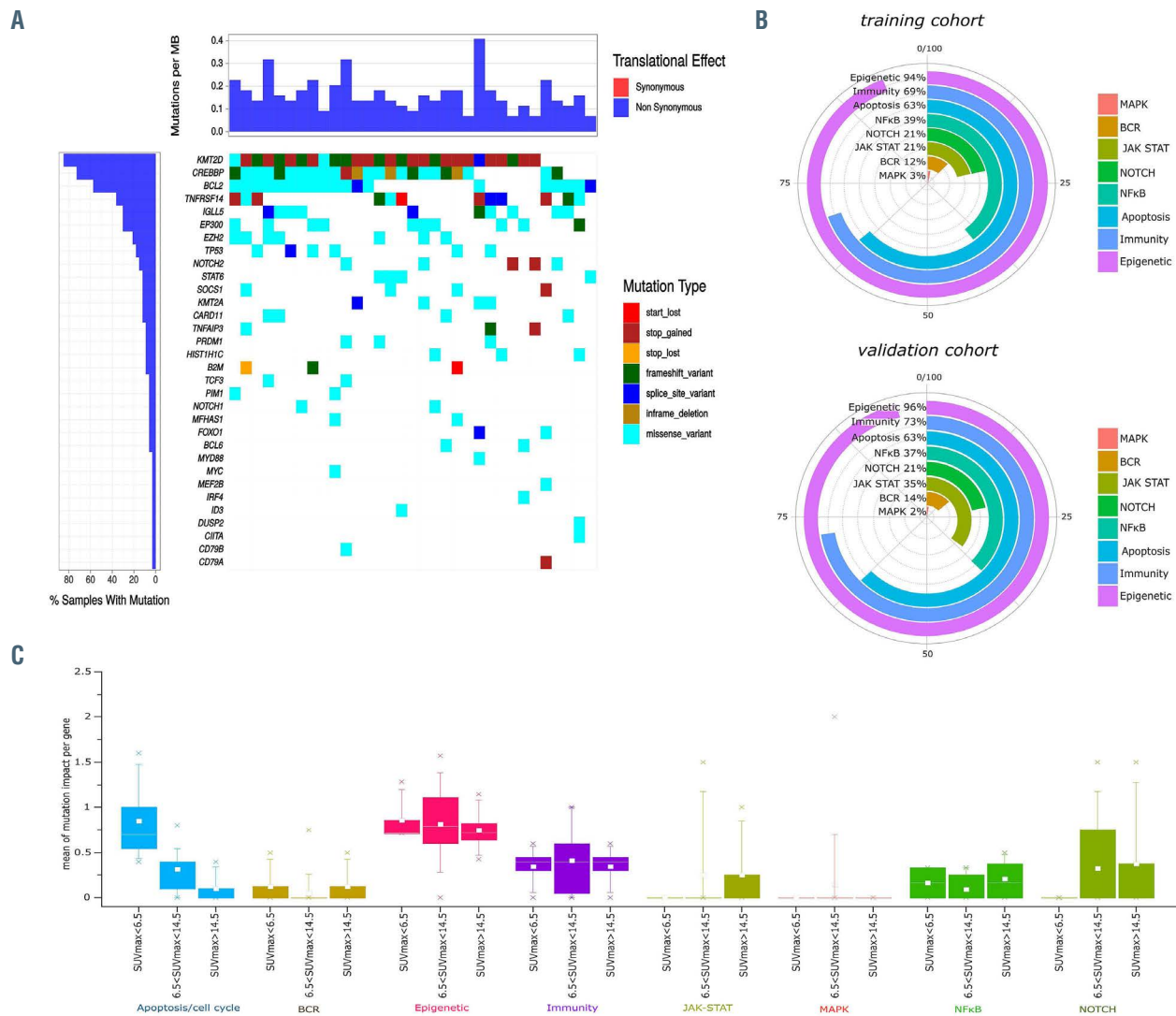


Figure 6. Molecular profiling of follicular lymphoma samples. (A) Heatmap of the most significantly mutated genes in follicular lymphoma (FL) samples from the training cohort (one column by sample, one line by gene). The colors refer to the type of mutation. (B) Circos plot illustrating the functional pathways involved in FL genomic abnormalities in the training (upper panel, n=33) and validation (lower panel, n=18) cohorts. The percentages refer to the frequency of alterations in the respective pathways. (C) Histogram showing the frequency of impaired functional pathways according to whole body maximum standardized uptake (SUV_{max}) levels.

patients. We also found an association between high SUV_{max} levels and tumor cell proliferation, but not with the cell content in the tumor microenvironment. Proliferative tumor cells are enriched in *FOXO1* mutations, which could explain their resistance to anti-CD20 therapy and subsequent poorer patient outcomes. The integrative approach used here could be applied in a multi-site lymph node analysis to further clarify the biological heterogeneity of FL and its relationship with functional imaging patterns.

Disclosures

CR has received a research grant from Roche and personal fees as well as non-financial support from Janssen, Roche, Takeda; ROC has received research grant from Gilead and Takeda and personal fees and non-financial support from Janssen, Roche, Takeda, Merck/BMS, Abbvie and Amgen. The other authors declare no competing interests.

Contributions

CR, PG, CL and CB designed the experimental strategy,

organized the experiments and collected and analyzed the data; CR, PG, PB, LY, LO and CG provided clinical data for the patients included in the series; SK performed analyses of PET-FDG; TF and JG performed statistical analyses; MT generated SES and performed analysis by data mining with CR, CB, JJF and CL; CL selected FL biopsies, performed and analyzed IHC and t-NGS experiments helped by PG, SP, SE, SR, LM, and CS; ROC, NA and DMF provided experimental advice; CR, JJF, CL and CB wrote the manuscript with advice from AS, CK, CL, MT, LY, PG. All authors discussed and approved the manuscript.

Acknowledgements

The authors would like to thank Nathalie Van-Acker (immunochemistry staining, Dept. of Pathology, IUCT-O, Imag'in Plateform, Toulouse), Frédéric Escudié and David Grand (NGS analysis, Dept. of Pathology, IUCT-O, Toulouse, Karin Gordien (Registre des Cancers du Tarn, Albi), Sophie Périés (CRB CHU Toulouse). We also thank Suzanne Rankin from the Dijon-Bourgogne University Hospital for proofreading the manuscript.

Funding

This work was supported in part by institutional grants from INSERM, Université Paul Sabatier and CNRS, Institut Claudius Regaud CLCC (contract R20027BB, CIEL) the Laboratoire

d'Excellence Toulouse Cancer (TOUCAN) (contract ANR11-LABX) and the Programme Hospitalo-Universitaire en Cancérologie CAPTOR (contract ANR11-PHUC0004). CR obtained a grant from ITMO Cancer Plan Cancer 2014-2019.

References

- Sarkozy C, Maurer MJ, Link BK, et al. Cause of death in follicular lymphoma in the first decade of the rituximab era: a pooled analysis of French and US cohorts. *J Clin Oncol*. 2019;37(2):144-152.
- Dada R. Diagnosis and management of follicular lymphoma: a comprehensive review. *Eur J Haematol* 2019;103(3):152-163.
- Casulo C, Byrtek M, Dawson KL, et al. Early relapse of follicular lymphoma after rituximab plus cyclophosphamide, doxorubicin, vincristine, and prednisone defines patients at high risk for death: an Analysis from the National LymphoCare Study. *J Clin Oncol*. 2015;33(23):2516-2522.
- Bodet-Milin C, Kraeber-Bodéré F, Moreau P, Campion L, Dupas B, Le Guillou S. Investigation of FDG-PET/CT imaging to guide biopsies in the detection of histological transformation of indolent lymphoma. *Haematologica*. 2008;93(3):471-472.
- Trotman J, Barrington SF, Belada D, et al. Prognostic value of end-of-induction PET response after first-line immunochemotherapy for follicular lymphoma (GALLIUM): secondary analysis of a randomised, phase 3 trial. *Lancet Oncol*. 2018;19(11):1530-1542.
- Meignan M, Cottreau AS, Versari A, et al. Baseline metabolic tumor volume predicts outcome in high-tumor-burden follicular lymphoma: a pooled analysis of three multicenter studies. *J Clin Oncol*. 2016;34(30):3618-3626.
- Bailly C, Carlier T, Berriolo-Riedinger A, et al. Prognostic value of FDG-PET in patients with mantle cell lymphoma: results from the LyMa-PET Project. *Haematologica*. 2020;105(1):e33-e36.
- Strati P, Ahmed MAA, Fowler N, et al. Pre-treatment maximum standardized uptake value predicts outcome after frontline therapy in patients with advanced stage follicular lymphoma. *Haematologica*. 2020;105(7):1907-1913.
- Dave SS, Wright G, Tan B, et al. Prediction of survival in follicular lymphoma based on molecular features of tumor-infiltrating immune cells. *N Engl J Med*. 2004;351(21):2159-2169.
- Laurent C, Champi K, Gravelle P, et al. Several immune escape patterns in non-Hodgkin's lymphomas. *Oncoimmunology*. 2015;4(8):e1026530.
- Huet S, Tesson B, Jais J-P, et al. A gene-expression profiling score for prediction of outcome in patients with follicular lymphoma: a retrospective training and validation analysis in three international cohorts. *Lancet Oncol*. 2018;19(4):549-561.
- Pastore A, Jurinovic V, Kridel R, et al. Integration of gene mutations in risk prognostication for patients receiving first-line immunochemotherapy for follicular lymphoma: a retrospective analysis of a prospective clinical trial and validation in a population-based registry. *Lancet Oncol*. 2015;16(9):1111-1122.
- Swerdlow SH, Campo E, Pileri SA, et al. The 2016 revision of the World Health Organization classification of lymphoid neoplasms. *Blood*. 2016;127(20):2375-2390.
- Kanoun S, Tal I, Berriolo-Riedinger A, et al. Influence of software tool and methodological aspects of total metabolic tumor volume calculation on baseline [18F]FDG PET to predict survival in Hodgkin lymphoma. *PLoS One*. 2015;10(10):e0140830.
- Laurent C, Guérin M, Frenois F-X, et al. Whole-slide imaging is a robust alternative to traditional fluorescent microscopy for fluorescence in situ hybridization imaging using break-apart DNA probes. *Hum Pathol*. 2013;44(8):1544-1555.
- Péricart S, Tosolini M, Gravelle P, et al. Profiling immune escape in Hodgkin's and diffuse large B-cell lymphomas using the transcriptome and immunostaining. *Cancers*. 2018;10(11):415.
- Evrard SM, Péricart S, Grand D, et al. Targeted next generation sequencing reveals high mutation frequency of CREBBP, BCL2 and KMT2D in high-grade B-cell lymphoma with MYC and BCL2 and/or BCL6 rearrangements. *Haematologica*. 2019;104(4):e154-e157.
- Vendrell JA, Grand D, Rouquette I, et al. High-throughput detection of clinically targetable alterations using next-generation sequencing. *Oncotarget*. 2017;8(25):40345-40358.
- Shuster JJ. Median follow-up in clinical trials. *J Clin Oncol*. 1991;9(1):191-192.
- Therneau T. 2020. A package for survival analysis in R. R package version 3.2-3 <https://CRAN.R-project.org/package=survival>.
- Terry M, Therneau, Patricia M. Grambsch. Modeling survival data: extending the Cox Model. A package for survival analysis in R. R package version 3.2-3, at <https://CRAN.R-project.org/package=survival>. New York: Springer. 2000.
- Benjamini, Y, Hochberg, Y. Controlling the false discovery rate - a practical and powerful approach to multiple testing. *J R Stat Soc Ser B Methodol*. 1995;57:289-300.
- Reshef DN, Reshef YA, Finucane HK, et al. Detecting novel associations in large data sets. *Science*. 2011;334(6062):1518-1524.
- Tosolini M, Algans C, Pont F, Ycart B, Fourmié J-J. Large-scale microarray profiling reveals four stages of immune escape in non-Hodgkin lymphomas. *Oncoimmunology*. 2016;5(7):e1188246.
- Salles G, Seymour JF, Offner F, et al. Rituximab maintenance for 2 years in patients with high tumour burden follicular lymphoma responding to rituximab plus chemotherapy (PRIMA): a phase 3, randomised controlled trial. *Lancet*. 2011;377(9759):42-51.
- Ashburner M, Ball CA, Blake JA, et al. Gene ontology: tool for the unification of biology. The Gene Ontology Consortium. *Nat Genet*. 2000;25(1):25-29.
- Fabregat A, Sidiropoulos K, Garapati P, et al. The Reactome pathway Knowledgebase. *Nucleic Acids Res*. 2016;44(D1):D481-487.
- Rummel MJ, Al-Batran SE, Kim S-Z, et al. Bendamustine plus rituximab is effective and has a favorable toxicity profile in the treatment of mantle cell and low-grade non-Hodgkin's lymphoma. *J Clin Oncol*. 2005;23(15):3383-3389.
- Batlevi CL, Sha F, Alperovich A, et al. Positron-emission tomography-based staging reduces the prognostic impact of early disease progression in patients with follicular lymphoma. *Eur J Cancer*. 2020;126:78-90.
- Alobthani G, Romanov V, Isohashi K, et al. Value of 18F-FDG PET/CT in discrimination between indolent and aggressive non-Hodgkin's lymphoma: A study of 328 patients. *Hell J Nucl Med*. 2018;21(1):7-14.
- Schöder H, Noy A, Gönen M, et al. Intensity of 18 Fluorodeoxyglucose uptake in positron emission tomography distinguishes between indolent and aggressive non-Hodgkin's lymphoma. *J Clin Oncol*. 2005;23(21):4643-4651.
- Xerri L, Huet S, Venstrom JM, et al. Rituximab treatment circumvents the prognostic impact of tumor-infiltrating T-cells in follicular lymphoma patients. *Hum Pathol*. 2017;64:128-136.
- Bachy E, Seymour JF, Feugier P, et al. Sustained progression-free survival benefit of rituximab maintenance in patients with follicular lymphoma: long-term results of the PRIMA Study. *J Clin Oncol*. 2019;37(31):2815-2824.
- Barrington SF, Trotman J, Sahin D, et al. Baseline PET-derived metabolic tumor volume metrics did not predict outcomes in follicular lymphoma patients treated with first-line immunochemotherapy and antibody maintenance in the phase III GALLIUM study. *Blood*. 2018;132(Suppl 1):S2882-2882.
- Falchi L, Ferrajoli A, Jacobs I, Nava-Parada P. An evidence-based review of anti-CD20 antibody-containing regimens for the treatment of patients with relapsed or refractory chronic lymphocytic leukemia, diffuse large B-cell lymphoma, or follicular lymphoma. *Clin Lymphoma Myeloma Leuk*. 2018;18(8):508-518.
- Rushton CK, Arthur SE, Alcaide M, et al. Genetic and evolutionary patterns of treatment resistance in relapsed B-cell lymphoma. *Blood Adv*. 2020;4(13):2886-2898.
- Jurinovic V, Kridel R, Staiger AM, et al. Clinicogenetic risk models predict early progression of follicular lymphoma after first-line immunochemotherapy. *Blood*. 2016;128(8):1112-1120.
- Pyrzynska B, Dwojak M, Zerrouqi A, et al. FOXO1 promotes resistance of non-Hodgkin lymphomas to anti-CD20-based therapy. *Oncoimmunology*. 2018;7(5):e1423183.
- Araf S, Wang J, Korfi K, et al. Genomic profiling reveals spatial intra-tumor heterogeneity in follicular lymphoma. *Leukemia*. 2018;32(5):1261-1265.